Journal of Medicinal Chemistry

pubs.acs.org/jmc

Article

A New Protractor Potentiates Glucagon-Like Peptide 1 with Slow-Release Depot and Long-Term Action

Weina Jing, Lei Peng, Shiwei Song, Jiaqi Liu, and Wanyi Tai*

Cite This: https://doi.org/10.1021/acs.jmedchem.4c02970

Read Online

ACCESS | Metrics & More | Article Recommendations | Supporting Information

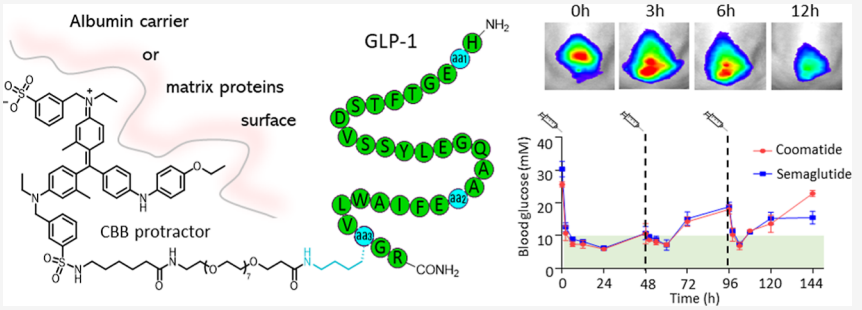

ABSTRACT: Bioactive peptides display a number of favorable features as therapeutics, but their usage is challenging due to the low metabolic stability and rapid renal clearance. The small-molecule protractor, which functions by the noncovalent binding with serum albumin and protection against systemic clearance, is an attractive tool to elongate peptides' half-life. Herein, we investigated coomassie brilliant blue (CBB) as a new protractor for the half-life extension of clinically relevant glucagon-like peptide 1 (GLP-1). A series of GLP-1 analogues differentiating with CBB linkers and acylation positions are described. One particularly interesting analogue (coomatide 13) exhibits sub-picomolar potency in vitro and long-term control of glucose homeostasis in mice. A protraction mechanism study reveals that CBB has a high affinity to albumin and pan-interaction with other matrix proteins, enabling to protract peptides in both systemic circulation and the subcutaneous depot. Our study demonstrates that the specific affinity to albumin is not a prerequisite for peptide protraction, and pan-binders might be advantageous.

INTRODUCTION

Bioactive peptides are naturally produced by many organisms and serve as hormones to regulate biological functions at a diverse array of physiological processes.[1] Because of this, bioactive peptides generally display high potency, good selectivity, and low toxicity, which are ideal as therapeutic leads.[2,3] At the same time, the display technologies—which include phage display, mRNA display, and bead screening system—provide a state-of-the-art approach to discovering new functional peptides beyond natural sources.[4,5] The screening campaigns in academia and the pharmaceutical industry have led to the identification of numerous peptides that display diverse pharmacological activities such as tumor homing, kinase inhibition, pathway blockade, and receptor interaction.[6−8] The booming research in peptides can be reflected by the current pipeline landscape, where more than 150 peptides enter clinical development and another 400−600 peptides undergo preclinical studies.[9,10]

Despite the importance of bioactive peptides as drug candidates, their limitations in pharmacokinetics (PK) should be recognized.[11,12] As small-sized biologics, peptides can be rapidly cleaned out from the circulation by fast renal filtration through glomeruli of the kidney, typically with half-lives of less than an hour.[13,14] This shortcoming dramatically limits the bioavailability of peptide drugs, especially those that require keeping action over an extended period. A number of strategies have been developed to prolong the circulation half-lives and improve peptide PK profiles.[15−17] This is exemplified by the decade-long pursuit of long-acting antidiabetic peptide, glucagon-like peptide 1 (GLP-1), by pharmaceutical scientists.[18] GLP-1 is an endogenous peptide hormone secreted by intestinal enteroendocrine L-cells following nutrient ingestion. It can rapidly and potently stimulate insulin secretion, a well-known action beneficial to type-2 diabetes treatment. The development of GLP-1 occurred during the 1990s when the GLP-1 peptide was found to have a half-life as short as 2 min.[19] The following studies have extended the half-life over 1 week and produced 6 marketed GLP-1 drugs by strategies like sequence modification, attachment of fatty acid to peptide, fusion with carrier proteins albumin or fragment crystallizable

Received: December 3, 2024
Revised: February 21, 2025
Accepted: March 11, 2025

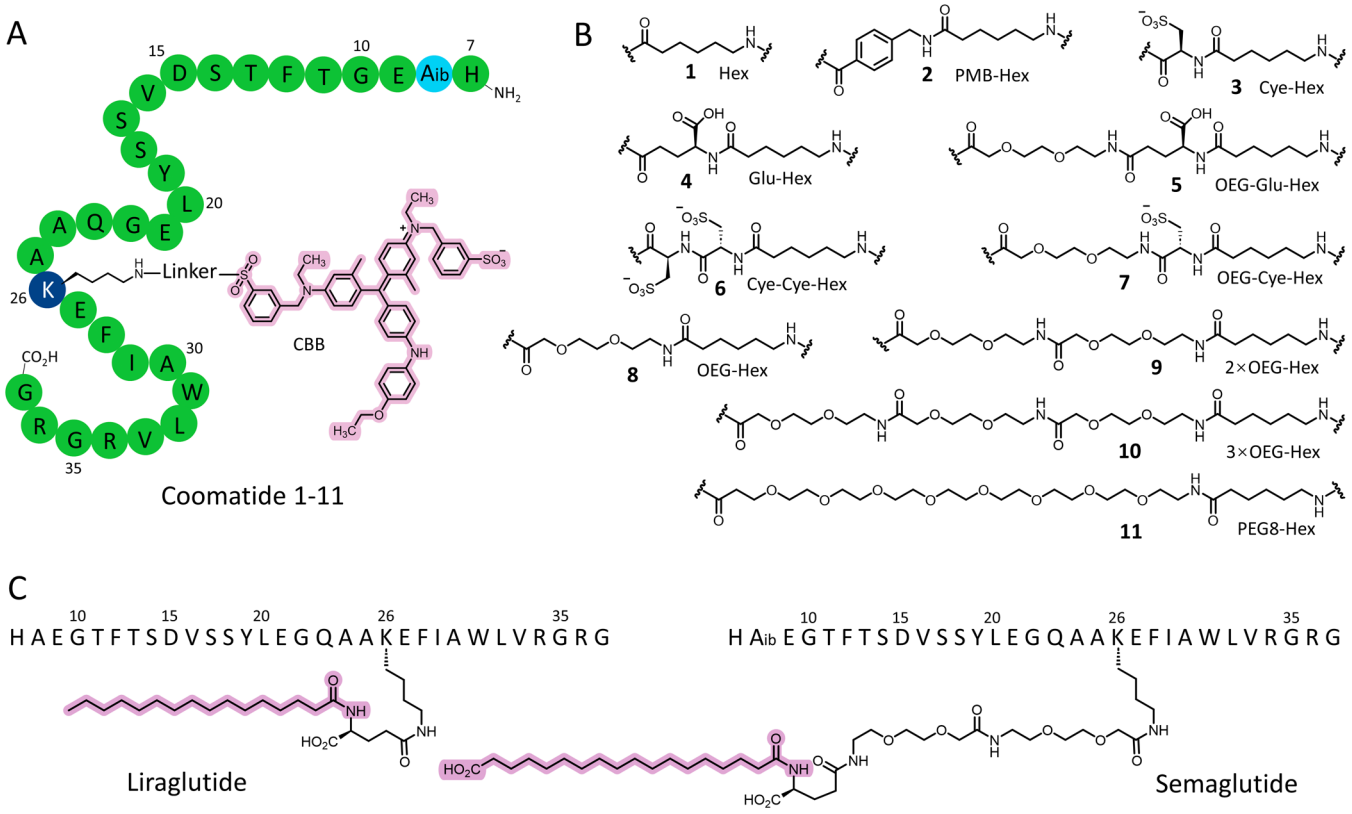

Figure 1. Schematic representation of coomatides 1−11 in comparison to liraglutide and semaglutide. (A) Structural schematic of coomatide showing peptide sequence, protractor CBB, and linkage. Aib: α-aminoisobutyric acid. (B) The chemical structures of linkers used in coomatides 1−11. (C) Molecular structures of FDA-approved liraglutide and semaglutide. The protracting molecules are highlighted in light purple.

(Fc) domain of antibody, PEGylation, and formulation with microsphere particles.[18] The ongoing efforts focus on the development of once-monthly GLP-1 analogues and more effective methods for oral administration.[20,21]

Among all of the half-life extension strategies, the small-molecule protractor approach is the most shining. Compared to other peptide carriers, the protractor is portable in size, easy to synthesize, low immune risk, and compatible with oral and subcutaneous (SC) routes.[22] The long-chain fatty diacids, such as C18 and C20 diacids, are the only known small-molecule protractors for peptides in the clinic. They have been used by FDA-approved peptides such as semaglutide (using C18 diacid), tirzepatide (using C20 diacid), insulin icodec (using C20 diacid), and many other clinical pipelines.[23−26] These fatty diacid protractors are hydrophobic molecules and show moderate binding affinity to human serum albumin (HSA) (K_D 0.6−2.0 μM).[27] When they are conjugated to the side chain of a lysine residue as a protraction moiety, GLP-1 peptide can attach piggy-back on albumin to obtain a very long residence time in blood circulation, given that albumin is the most abundant protein in plasma (40 mg/mL) and has a half-life of 19 days in humans.[28] Despite the attraction of long-chain fatty diacids, the low solubility in aqueous solution and relatively weak affinity to albumin can be significant limitations.[29,30] There is considerable scientific interest in the identification of new small-molecule protractors that display a better solubility and more stable interaction with albumin.

In this work, we set out to evaluate coomassie brilliant blue (CBB) as a new protractor to potentiate GLP-1 peptide efficacy in type 2 diabetes therapy. CBB is a water-soluble dye commonly used in biochemistry laboratories for protein staining. It is also a small-molecule drug in clinical use under the trade name brilliant peel for retinal surgery and a candidate to treat spinal injuries.[31] CBB is well-known for its ability to bind noncovalently with proteins via the van der Waals force and heteropolar interaction.[32] Its affinity for albumin is stronger than that of C18 diacid, but the interaction is not specific, which means that CBB may jump off albumin when it encounters other proteins. However, albumin, as the most abundant protein in plasma (~60 wt %), likely could possess CBB in circulation and be able to fulfill its role to carry the CBB-protracted peptides. Herein, we describe a series of CBB-protracted GLP-1 analogues and show that CBB is competitive with C18 diacid in peptide protraction. The best candidate coomatide 13 demonstrates a better PK profile and efficacy than semaglutide without compromising the peptide solubility. We also reveal that the CBB protractor can interact reversibly with the extracellular matrix proteins, for example, collagen under the skin after SC injection, thus generating a slow-release depot to prolong the GLP-1 effect further. Compared to C18 diacid, the new protractor CBB takes into account all the limitations in the area, including albumin binding avidity, aqueous solubility, chemical safety, easy synthesis, and vast availability, which may merit the peptide drug development in the future.

RESULTS

Linker Optimization for CBB Protractor. The design of coomatides is mainly inspired by semaglutide, which is regarded as a milestone in the development of GLP-1 peptide drugs.[23] Semaglutide is derived from the once-daily liraglutide but suitable for once-weekly administration. It has several

https://doi.org/10.1021/acs.jmedchem.4c02970
J. Med. Chem. XXXX, XXX, XXX−XXX

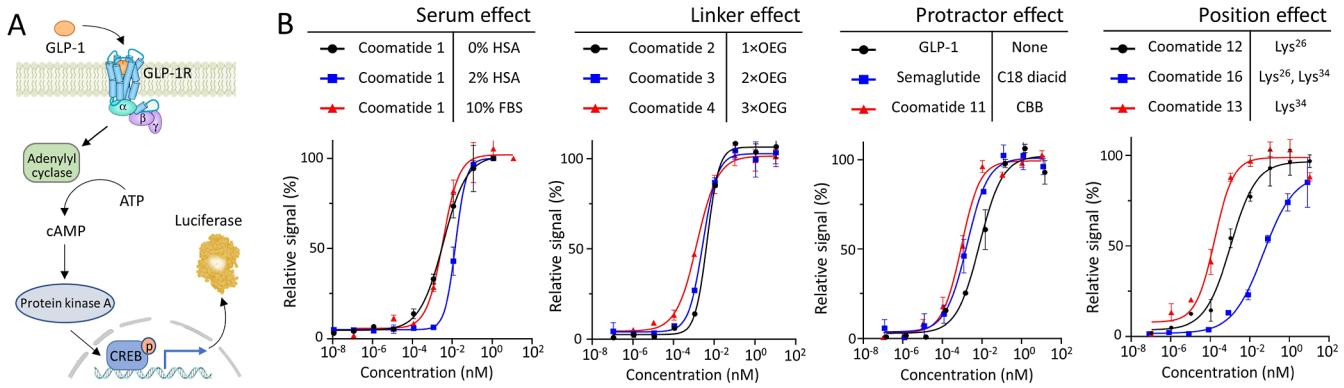

Figure 2. In vitro function assay of GLP-1 peptide analogues. (A) A diagram illustrating the GLP-1R signaling pathway coupled with CRE-luciferase reporter in the HEK293 stable cell line. (B) Activity profiles of some typical peptide analogues concerning the factors such as serum concentration, linker length, protractor structure, and acylation position. The activity was determined in the GLP-1R expressing stable HEK293 cells. All data are presented as the mean ± SD (n = 3).

Table 1. Table Summarizing the EC_{50} Values of Coomatides 1−11 and Comparing to GLP-1 Naked Peptide, Semaglutide, and Liraglutide

						EC50 (pM)[a]			
analogue	modification	protractor	linkage	acylatin position	C-term	0% HSA	2% HSA	10% FBS	ratio 2%/0% HSA
GLP-1(7−37)	Aib^8, Arg^{34}	none	none	none	$-CO_2H$	30.67 ± 14.71	28.85 ± 12.46	8.32 ± 0.72	0.94
semaglutide	Aib^8, Arg^{34}	C18 diacid	Glu-2xOEG	Lys^{26}	$-CO_2H$	0.13 ± 0.01	3.87 ± 2.00	1.88 ± 0.13	29.8
liraglutide	Arg^{34}	C16	Glu	Lys^{26}	$-CO_2H$	1.07 ± 0.06	9.05 ± 0.15	2.56 ± 0.43	8.46
coomatide1	Aib^8, Arg^{34}	CBB	Hex	Lys^{26}	$-CO_2H$	3.75 ± 0.18	8.82 ± 6.01	3.55 ± 0.11	2.35
coomatide2	Aib^8, Arg^{34}	CBB	PMB-Hex	Lys^{26}	$-CO_2H$	1.08 ± 0.07	3.22 ± 0.11	4.20 ± 0.18	2.98
coomatide3	Aib^8, Arg^{34}	CBB	Cye-Hex	Lys^{26}	$-CO_2H$	1.12 ± 0.02	8.86 ± 1.47	4.08 ± 0.17	7.91
coomatide4	Aib^8, Arg^{34}	CBB	Glu-Hex	Lys^{26}	$-CO_2H$	1.17 ± 0.06	9.10 ± 0.06	2.92 ± 0.77	7.78
coomatide5	Aib^8, Arg^{34}	CBB	OEG-Glu-Hex	Lys^{26}	$-CO_2H$	0.63 ± 0.03	3.29 ± 0.1	4.99 ± 0.19	5.22
coomatide6	Aib^8, Arg^{34}	CBB	Cye-Cye-Hex	Lys^{26}	$-CO_2H$	1.66 ± 0.01	7.08 ± 0.43	6.98 ± 0.63	4.27
coomatide7	Aib^8, Arg^{34}	CBB	OEG-Cye-Hex	Lys^{26}	$-CO_2H$	1.13 ± 0.02	4.25 ± 0.16	1.16 ± 0.54	3.76
coomatide8	Aib^8, Arg^{34}	CBB	OEG-Hex	Lys^{26}	$-CO_2H$	3.35 ± 0.04	14.50 ± 0.17	4.58 ± 0.06	4.33
coomatide9	Aib^8, Arg^{34}	CBB	2xOEG-Hex	Lys^{26}	$-CO_2H$	0.79 ± 0.03	3.94 + 0.12	2.93 ± 0.08	4.99
coomatide10	Aib^8, Arg^{34}	CBB	3xOEG-Hex	Lys^{26}	$-CO_2H$	0.83 ± 0.43	4.31 ± 0.02	1.46 ± 0.04	5.20
coomatide11	Aib^8, Arg^{34}	CBB	PEG8-Hex	Lys^{26}	$-CO_2H$	0.16 ± 0.01	2.44 ± 0.58	0.93 ± 0.03	15.25

[a]The EC_{50} assay was performed using HEK293/CRE-Luc/GLP-1R stable cells in the assay buffer containing 0% HSA, 2% HSA, or 10% FBS. Data are expressed as the mean ± SD (n = 3).

important features that are important in GLP-1 derivatization: semaglutide has a high homogeneity to native GLP-1 in sequence, which helps avoid the immunogenicity response seen in exenatide and taspoglutide; the N-terminal Ala^8 is substituted by Aib^8 to protect against dipeptidyl peptidase 4 (DPP-4) degradation, but negligible to the bioactivity of GLP-1 peptide; the site of acrylation is chosen at Lys^{26}.[33,34] In order to accurately evaluate the potential of the CBB protractor, the key criterion of design is to keep the peptide structurally the same as semaglutide and only replace the C18 diacid protractor with the CBB of different linkers (Figure 1A). A series of linkers with different lengths and residues were prepared. The linkers range from 6 to 34 atoms in length and cover the residue groups including alkyl carbons, phenyl groups, carboxylic acids, sulfonic acids, and PEGs, as shown in Figure 1B.

The structure−activity relationship (SAR) of the analogues (coomatides 1−11, obtained via routes in Scheme S1) was investigated by a functional assay employing the engineered HEK293 cells (Figure 2A). This stable cell line has the constitutive expression of the human GLP-1 receptor (GLP-1R) and carries a firefly luciferase gene under the control of a cAMP response element (CRE). Activation of GLP-1R by GLP-1 analogues in these cells triggers the intracellular accumulation of cAMP, which can be monitored by measuring the luciferase activity. Figure 2B shows examples of the dose−response curves for a few selected analogues. All peptides tested are full agonists and induce luciferase activity in a dose-dependent manner (Figure S1). The most apparent observation is the negative impact of serum (2% vs 0% HSA) on the potency of GLP-1 analogues (Figure S2). It is understandable, considering the circumstance that a peptide associated with serum protein is usually unavailable for binding to GLP-1R. The presence of 10% fetal bovine serum (FBS), the most common serum concentration in cell culture, also causes a decrease in potency, but less severe than 2% HSA, likely due to its low protein level (~0.5%) and nutrient-rich environment during the assay. Besides the serum effect, there is a general tendency to improve potency under serum-containing conditions by increasing the linker length. For example, potency is a 3.2-fold increase when the linker is prolonged from 1 × OEG to 3 × OEG, and the difference is the highest of

https://doi.org/10.1021/acs.jmedchem.4c02970
J. Med. Chem. XXXX, XXX, XXX−XXX

Scheme 1. The Semi-Synthesis Approach to Coomatides from Recombinant GLP-1 Peptides

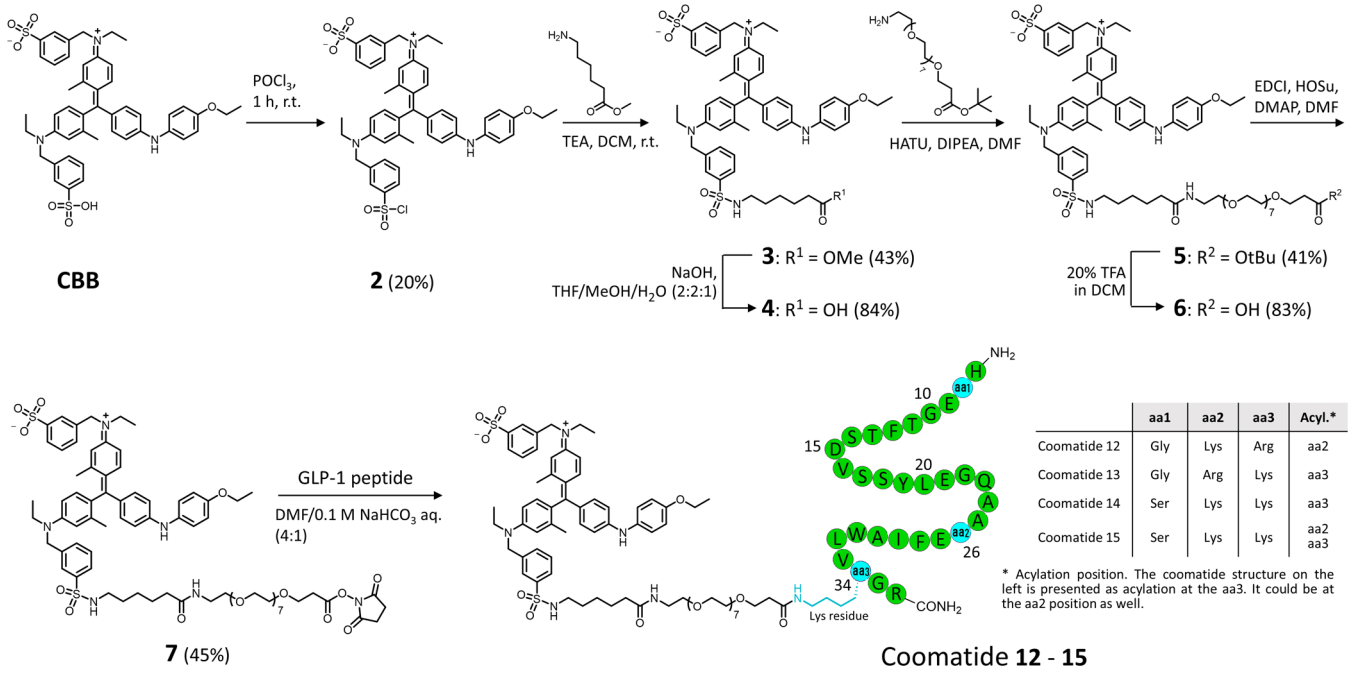

Table 2. Coomatide Analogues 12−15 with the PEG8 Linkage and Variable Peptide Sequences

analogue	modification	protractor	linkage	acylatin position	C-term	EC50 (pM)[a] 0% HSA	EC50 (pM)[a] 2% HSA	EC50 (pM)[a] 10% FBS	ratio 2%/0% HSA
GLP-1(9−36)	none	none	none	none	$-CONH_2$	no effect	no effect	no effect	
(G8R34)GLP-1(7−36)	Gly^8, Arg^{34}	none	none	none	$-CONH_2$	66.90 ± 15.53	74.83 ± 36.68	18.90 ± 0.23	1.12
(G8R26)GLP-1(7−36)	Gly^8, Arg^{26}	none	none	none	$-CONH_2$	62.79 ± 32.67	84.21 ± 42.21	16.08 ± 0.11	1.34
(S8)GLP-1(7−36)	Ser^8	none	none	none	$-CONH_2$	50.20 ± 6.39	60.95 ± 5.24	42.44 ± 0.61	1.21
coomatide12	Gly^8, Arg^{34}	CBB	PEG8-Hex	Lys^{26}	$-CONH_2$	1.11 ± 0.15	5.11 ± 1.03	1.19 ± 0.11	4.60
coomatide13	Gly^8, Arg^{26}	CBB	PEG8-Hex	Lys^{34}	$-CONH_2$	0.37 ± 0.05	1.99 ± 0.01	0.21 ± 0.02	5.38
coomatide14	Ser^8	CBB	PEG8-Hex	Lys^{34}	$-CONH_2$	0.33 ± 0.11	0.84 ± 0.15	3.96 ± 0.41	2.55
coomatide15	Ser^8	CBB	PEG8-Hex	Lys^{26}, Lys^{34}	$-CONH_2$	2.40 ± 0.91	12.01 ± 6.03	65.25 ± 16.57	5.00

[a]The EC_{50} assay was performed using HEK293/CRE-Luc/GLP-1R stable cells in the assay buffer containing 0% HSA, 2% HSA, or 10% FBS. Data are expressed as the mean ± SD (n = 3).

5-fold with coomatide 11, which has the longest linker (PEG8). It is interesting to observe that the graft of protractor moieties has a positive effect on the potency of peptides. The result is surprising, but in accordance with the earlier report which concludes that the unspecific adhesion of the protractor moiety to the GLP-1R surface might contribute to the peptide affinity to receptors and augment the potency.[23] It is noteworthy that the graft of CBB with GLP-1 peptide does not induce nonspecific activation of other GPCRs, for example, GLP-2R in our test, indicating the dominance of the peptide moiety in receptor recognition and activation (Figure S3).

As seen in Table 1, a series of linkers with the terminal acids are derivatized at Lys^{26} of GLP-1 with CBB. The acidic group is introduced to compensate for the loss of the sulfonic group of the CBB used for amide linkage. The addition of acidic residues, either carboxylic or sulfonic acids, compromises the potency, especially when multiple sulfonic acids are introduced. Although the length has a significant impact on potency, the linker composition is not considered to be important as there is no difference between the two longest linkers (coomatide 10 and coomatide 11). Because the PEG8 linker (coomatide 11) is commercially available and easy to obtain, it is decided to focus on it for further derivatization. It is worth noting that the linker length required for optimal activity of coomatide is much longer than that of semaglutide, which might be attributed to the protractors' difference in topology (C18 diacid itself is linear and flexible, whereas the configuration of CBB is crowded and rigid).

Potent Coomatide Derivatives with Feasibility of Scale-Up. After the linker optimization, a campaign was designed to conjugate CBB via the best linker but to vary the GLP-1 peptide sequences. The rationale is to obtain a coomatide structure that is feasible to scale up. Both semaglutide and our best analogue in Table 1 consist of a 31 amino acid peptide backbone and noncoded aminoisobutyric acid residues (Aib) at position 8. The synthetic routes are all

https://doi.org/10.1021/acs.jmedchem.4c02970
J. Med. Chem. XXXX, XXX, XXX−XXX

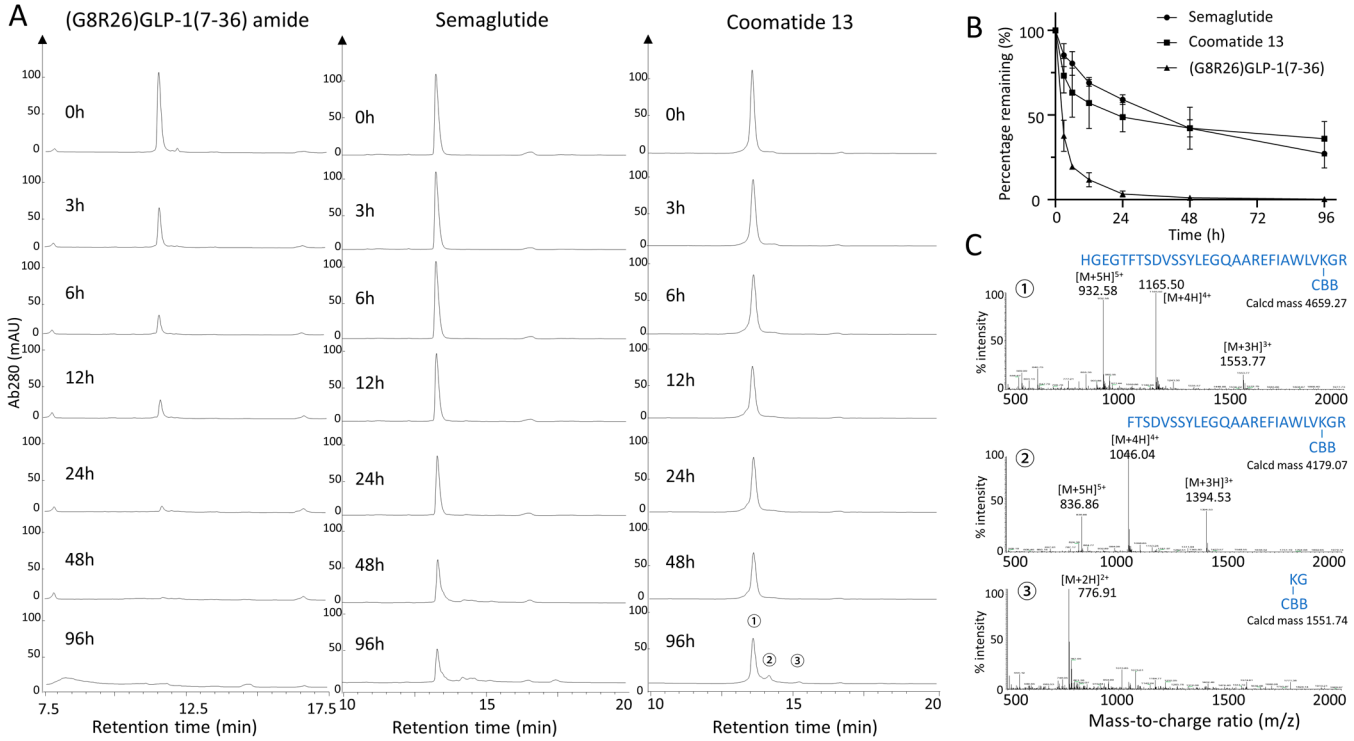

Figure 3. In vitro stability test of GLP-1 analogues in rat plasma. (A) The HPLC spectra of peptide analogues after incubation in rat plasma. (B) Stability profiles by plotting % peptide remaining against incubation time. (C) Mass spectra showing the metabolites after 96 h incubation with rat plasma. All tests were performed in triplicate and repeated with similar results.

based on solid-phase peptide synthesis, which leads to high production costs and low efficiency.[35] Recombinant technology is the most economical way to scale up peptide synthesis in industry.[36] To embrace this technology, three GLP-1 analogues with natural amino acid backbones were selected and derivatized at the Lys^{26} or Lys^{34} or both positions with a CBB protractor by a semisynthesis approach (Scheme 1). Gly^{8} and Ser^{8} were chosen to replace the non-coded Aib^{8} according to the previous reports.[37,38] Especially, Gly^{8} has been used by two FDA-approved GLP-1 drug, dulaglutide and albiglutide, both of which are designated to inject once weekly.[18] The peptide backbone has also been explored to shorten to 30 residues, along with a C-terminal amide for degradation resistance.

The in vitro potency assay revealed that the two naked peptides retain the bioactivity, but the Ser^{8}-bearing GLP-1, namely, (S8)GLP-1(7−36), displays a 2.5-fold decrease in potency, indicating the superiority of Gly^{8} over Ser^{8}. (Table 2). We decided to focus on these two peptides by CBB derivatization with the most promising linker, PEG8. It was observed that coomatide 13, a peptide derivatized on Lys^{34}, gave the highest potency with an EC50 value below 0.5 pM, which is 5 times stronger than its comparator coomatide 12 (derivatization on Lys^{26}) and 84 times stronger than its parent peptide (G8R26)GLP-1(7−36). This result is in line with the previous finding that the C-terminal part of GLP-1 involves less receptor binding and could be derivatized with no attenuation of potency.[33] Based on our result, derivatization at the distal end, for example, Lys^{34} in this case, seems advantageous, likely owing to its minimal disruption to the receptor activation. In this regard, coomatide 13 is selected as our candidate for the following study.

CBB Protractor Enhances Peptide Stability. In stability tests, candidate coomatide 13 is compared with its parent peptide (G8R26)GLP-1(7−36) and the positive control semaglutide. Peptide stability was evaluated in rat plasma and quantified by analysis of the peptide peak remaining over time on reverse-phase high performance liquid chromatography (RP-HPLC). At time zero, all three peptides produce single peaks, which correspond well to their intact peptide molecular mass (Figure 3A). Incubation in rat plasma at 37 °C for 96 h results in a huge difference in the peak area between the three peptides; (G8R26)GLP-1(7−36) completely loses its peak height. In contrast, 30% of intact semaglutide and 40% of coomatide 13 remain after 96 h incubation (Figure 3B). The degradation of (G8R26)GLP-1(7−36) follows first-order kinetics, with a calculated half-life of 50 min. The half-life of coomatide 13 is substantially longer (24 h) than naked peptide but shorter than semaglutide (36 h). The enhanced stability of semaglutide and coomatide can be attributed to the protractor moieties in the peptide side chains. These protractors protect the lysine residue and make the adjacent peptide bonds resistant to degradation. More importantly, it can recruit albumin from serum and bulk up the size of peptides, which may dramatically prolong its shelf life in serum. It is known that large proteins are less liable to degradation by proteases than small-sized peptides/proteins. In rat plasma, semaglutide and coomatide 13 exist mostly as a complex with albumin, exhibiting an apparent molecular weight (M_w) of ∼70 kDa, which is coherently more stable than the naked peptide (G8R26)GLP-1(7−36) (M_w 3.3 kDa).

The enzyme DPP-4 plays an important role in the degradation of native GLP-1 peptide.[38] To investigate whether it involves the degradation pathway, we analyzed the nascent peaks from coomatide 13 spectra by mass spectrometry (MS)

https://doi.org/10.1021/acs.jmedchem.4c02970
J. Med. Chem. XXXX, XXX, XXX−XXX

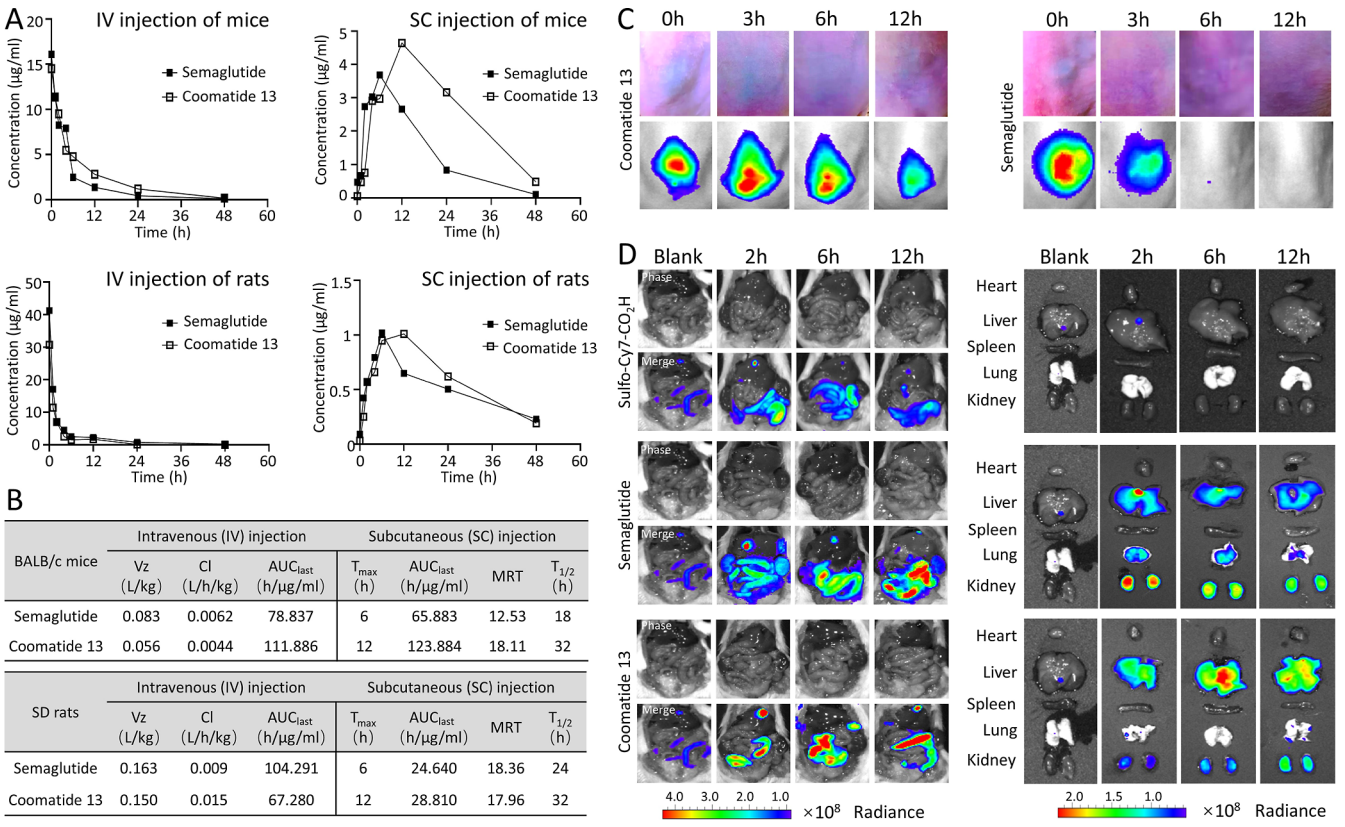

B

BALB/c mice	Intravenous (IV) injection			Subcutaneous (SC) injection			
	Vz (L/kg)	Cl (L/h/kg)	AUC_{last} (h/μg/ml)	T_{max} (h)	AUC_{last} (h/μg/ml)	MRT	$T_{1/2}$ (h)
Semaglutide	0.083	0.0062	78.837	6	65.883	12.53	18
Coomatide 13	0.056	0.0044	111.886	12	123.884	18.11	32

SD rats	Intravenous (IV) injection			Subcutaneous (SC) injection			
	Vz (L/kg)	Cl (L/h/kg)	AUC_{last} (h/μg/ml)	T_{max} (h)	AUC_{last} (h/μg/ml)	MRT	$T_{1/2}$ (h)
Semaglutide	0.163	0.009	104.291	6	24.640	18.36	24
Coomatide 13	0.150	0.015	67.280	12	28.810	17.96	32

Figure 4. PKs and biodistribution of peptide analogues in animal models. (A) The PK profiles in mice and rats following IV administration (left panels) or SC administration (right panels) of peptides. (B) A table showing the key PK parameters in BALB/c mice and SD rats. (C) The photo and fluorescence images showing the percutaneous absorption of peptides over time. Peptides were labeled with sulfo-Cy7, and the blue color under white light comes from the natural color of CBB. (D) NIR fluorescence tracking the biodistribution in mice following IV injection of sulfo-Cy7-labeled peptide analogues. The PK study was performed in triplicate (n = 3), and imaging analysis was repeated twice.

after 96 h incubation with rat plasma. Mass spectrometric analysis reveals that all the peaks are the truncated metabolites of coomatide 13, but the cleavage site is seen near the position Phe[12] (Figure 3C). With the increase of incubation time, lower molecular weight fragments, such as Lys(CBB)Gly and Lys(CBB), are detected, suggestive of a deep degradation of metabolites (Figure S4).

Protraction in the SC Depot and Systemic Circulation. The in vivo characterization of coomatide 13 starts with the evaluation of PKs in BALB/c mice and Sprague–Dawley (SD) rats. The in vivo half-life ($T_{1/2}$) of semaglutide has been reported to be greatly extended due to the protractor C18 diacid. In the present study, we observe a similar $T_{1/2}$ value (~3 h) of coomatide 13 to semaglutide in mice when administrated via the intravenous (IV) route (Figure 4A). However, the PK profile of coomatide 13 after the SC injection displays a half-life much longer than that of semaglutide ($T_{1/2}$ = 32 h vs 18 h). Moreover, a delayed T_{max} is seen in mice treated with coomatide 13 relative to semaglutide (T_{max} = 6 vs 12 h), which suggests a slow and measured release of coomatide 13 from the SC depot. Similar PK profiles were observed in SD rat models as well. In Figure 4B, the PK parameters of semaglutide and coomatide 13 are presented. The volume distribution of coomatide 13 after IV administration is 0.056 L/kg in mice and 0.150 L/kg in rats, respectively. Its values are slightly lower than those of semaglutide, indicating the fewer distributions in peripheral tissues. Body clearance of coomatide 13 is 0.0044 L/h/kg, 1.4 times lower than semaglutide, suggestive of the reduced clearance. However, the trend is reversed in SD rat models, in which we speculate that protractors might possess variable binding avidity to albumin of different species. This disparity also impacts the mean residence time of peptides in animal models following SC administration. Nevertheless, the observed SC bioavailability (AUC_{last}) of coomatide 13 is unaffected and higher than that of semaglutide in both animal models we tested. It is speculated that the slow release of coomatide 13 from the skin depot might increase the bioavailability of peptide, but further studies are required to conclude.

We then set up a tracking system for the cutaneous peptide release by labeling them with fluorescent sulfo-Cy7 dye and monitoring the absorption over time in mice. As depicted in Figure 4C, we found that coomatide 13 retains in the SC depot much longer than semaglutide. It takes an appropriate 3 h for most semaglutide to be taken up by skin, whereas a period over 12 h is required in the case of coomatide 13. Interestingly, the disappearance of cutaneous peptides coincides with the upward trend of the PK curves, indicating the translocation of peptides from skin to circulation. The biodistribution of peptides was then tracked in BALB/c mice following IV injection (Figure 4D). The intraoperative imaging reveals the high deposition of sulfo-Cy7-labeled peptides in bodies, but it is difficult to distinguish because the nonspecific background is high. We next tested the signals in the dissected organs, including the heart, liver, spleen, lung, and kidney. Both peptides express the elevated fluorescence in the liver and kidney, which may represent their metabolic pathway in vivo.

https://doi.org/10.1021/acs.jmedchem.4c02970
J. Med. Chem. XXXX, XXX, XXX−XXX

Different from coomatide 13, semaglutide also demonstrates distribution in the lung, which might be related to its lipidation status.

The PK data and tracking images shown above suggest that the protraction of the peptide by CBB not only takes place in the bloodstream but also in the SC depot after SC injection. It is hypothesized that the CBB moiety of coomatide might interact with the matrix proteins in the interstitium, which slows down the release and absorption by the vasculature. The interstitium is an interconnected, fluid-filled compartment, which surrounds vascular networks and has the ability to commute with intravascular fluid.[39] Its space is supported by the collagen skeleton, thus, very dynamic and malleable to accommodate a drug bolus. To explore the role of matrix proteins, we immobilized the collagen protein on the biosensors of octet bio-layer interferometry (BLI) and profiled the dissociation constant (K_D) values. The step-binding assay in Figure 5 shows that coomatide 13 can bind collagen as well as HSA, both with K_D values of around 0.5 μM. Its affinity to proteins is moderate but reversible, which enables the peptide traffic from the matrix protein to albumin and finally the GLP-1R. Unlike CBB, C18 diacid in semaglutide is a more specific protractor to HSA.[28] We did not obtain an accurate K_D value of semaglutide to HSA albumin but observed the apparent response to HSA in the step-binding curves. The response of semaglutide to collagen is neglectable. Altogether, our results demonstrate that the specific binding with albumin is not a prerequisite for protractors. Broad avidity instead might provide a bonus such as slow release that benefits the long-term action.

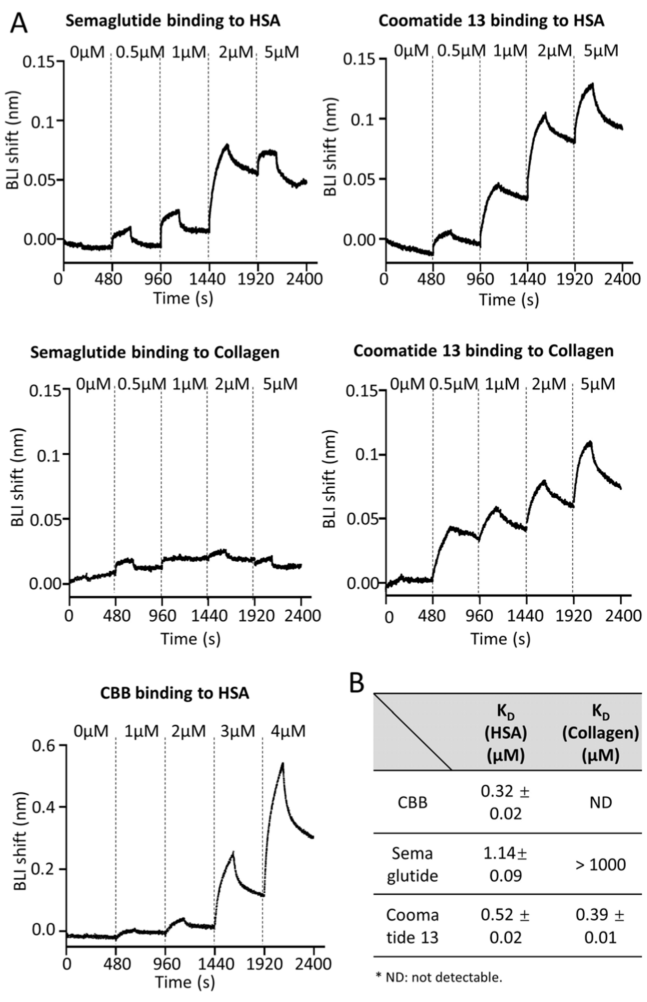

	K_D (HSA) (μM)	K_D (Collagen) (μM)
CBB	0.32 ± 0.02	ND
Semaglutide	1.14± 0.09	> 1000
Coomatide 13	0.52 ± 0.02	0.39 ± 0.01

Figure 5. Affinity assessment by BLI step-binding assay. (A) BLI sensorgrams for the binding of peptides (protractors) to the immobilized HSA and collagen protein on the AR2G biosensors. (B) A table summarizing the affinity K_D values (n = 3).

Glucose Control in Mouse Models of Type 2 Diabetes. The db/db mouse with type 2 diabetes was used in the in vivo evaluation of coomatide 13 for antidiabetic therapy. A dose−response study in Figure 6A reveals that the antihyperglycemic efficacy of coomatide 13 is dose-dependent, and the duration of action (blood glucose <10 mM) can reach up to 48 h. Calculated on the basis of AUC blood glucose during 0−96 h after dosing, we obtain an EC_{50} of 30 nmol/kg for coomatide 13. This value is much higher than the EC_{50} of semaglutide previously reported (2 nmol/kg), but the parallel studies of the two peptides with equal doses (Figure 6B,C) showed that they have similar antihyperglycemic efficacy in terms of potency and duration of action. Not surprisingly, their effects in the diabetes mouse model are much better than the naked GLP-1 peptide control and vehicle control.

The effect of GLP-1 analogues on glucose tolerance was studied in two experiments. The db/db mice were subjected to 16 h of fasting and then administered subcutaneously with either semaglutide or coomatide 13. Half an hour later, when those peptides were absorbed, the glucose solution (1.5 g/kg) was injected into mice via the intraperitoneal route. Data of the glucose excursion in Figure 6D shows that both semaglutide and coomatide 13 can well maintain the homeostasis of blood glucose. The oral glucose tolerance test reveals a similar effect of glucose control by both peptides (Figure 6E). To investigate the effect of repeat dosing, the db/db mice has full access to food but receives 100 nmol/kg GLP-1 peptides once every 48 h. As shown in Figure 6F, both semaglutide and coomatide 13 well control blood sugar levels below 10 mM for most of the first treatment cycle. However, their antihyperglycemic effects are less effective over time in the following cycles. Considering that semaglutide has been used for repeated administration by type-2 diabetes patients, our observation is surprising but can be explained by the limitation of the current db/db mice models, which are established by genetic predisposition and may not predict human treatment outcomes. In the glucose control experiments, we also observe a reduction of food intake by mice treated by coomatide 13 (Figure 6G), indicating the potential of the peptide in gastric emptying and obesity management.

DISCUSSION AND CONCLUSIONS

The long-term action is the major medical need of many therapeutic peptides.[40] The importance and urgency are extremely exemplified in the field of developing GLP-1 peptides.[18] Covalent attachment of a C16 fatty acid, known as lipidation, has been used to control the half-life of GLP-1 in the example of liraglutide.[33] It extends the half-life of GLP-1 to 13 h and supports a once-daily injection. Besides lipids, PEG and XTEN polymers have also been applied to prolong the systemic circulation of peptides in vivo.[18] Several candidates, for example, LY2428757 and VRS-859, have advanced to clinical testing for once-weekly administration.[41,42] The FDA-approved GLP-1 drugs albiglutide and dulaglutide represent another strategy in which GLP-1 is genetically fused with long-

https://doi.org/10.1021/acs.jmedchem.4c02970
J. Med. Chem. XXXX, XXX, XXX−XXX

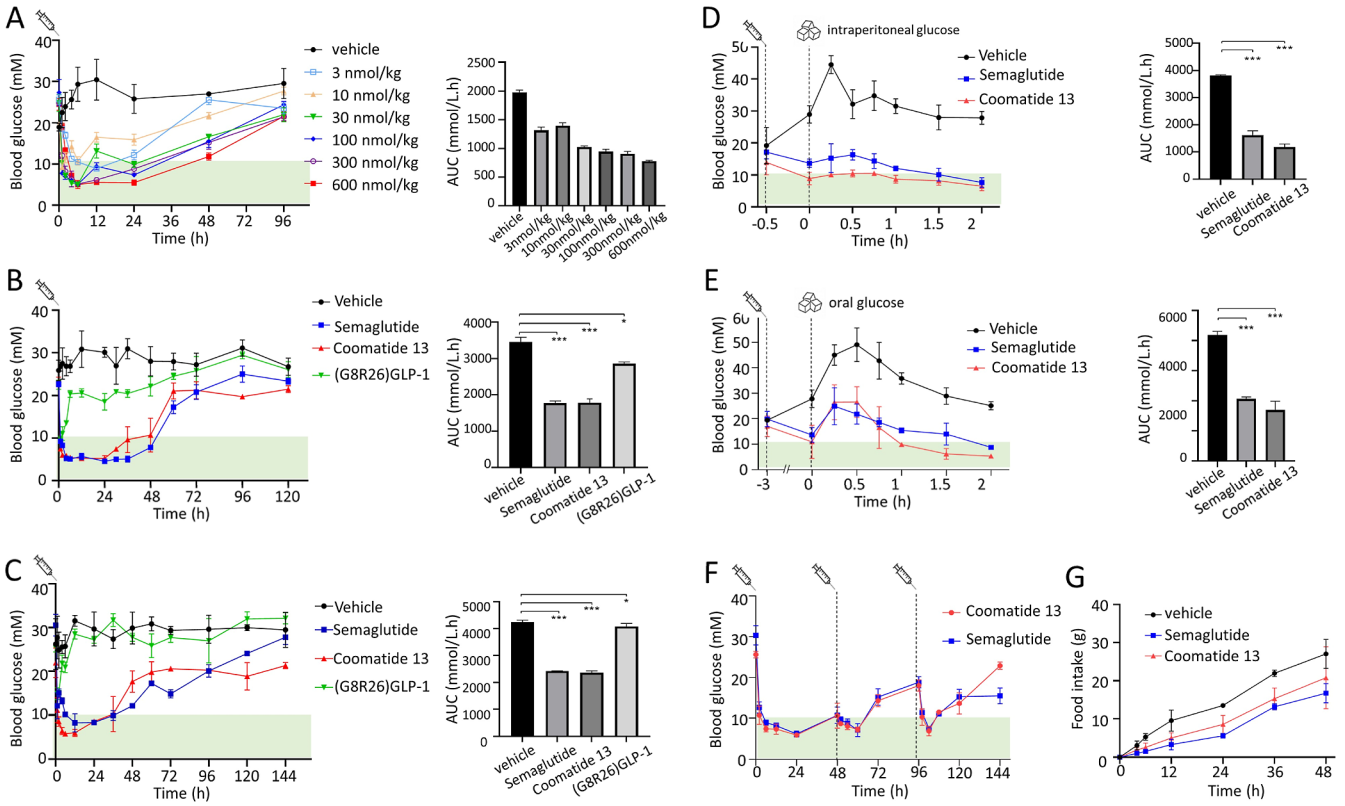

Figure 6. Glucose control of db/db mice by the protracted GLP-1 peptides. (A) Dose-dependent regulation of blood glucose levels by coomatide 13 ranging from 3 to 600 nmol/kg. (B) Single administration (SC) of a high dose (600 nmol/kg) of semaglutide or coomatide 13 to treat hyperglycemia. (C) Single dose of peptide analogues (100 nmol/kg) to control blood glucose in db/db mice via SC route. (D) Intraperitoneal glucose tolerance test after treatment with a single 100 nmol/kg dose of peptides. (E) Acute glucose tolerance test by challenging with 1.5 g/kg oral dose of glucose at 3 h after GLP-1 peptide administration. (F) Long-term antihyperglycemic evaluation by repeated doses of the peptide analogues. (G) Cumulative food intake of db/db mice treated by peptide analogues for 48 h. *$P < 0.05$, *** $P < 0.01$.

circulating carrier proteins (albumin and Fc) to achieve long-term action.[18]

Despite the diversity of strategies in half-life extension, the small-molecule protractor remains the most popular strategy to prolong the peptides' action, likely due to its low cost, portability, and low immune risk.[22] With the booming of semaglutide, there is a growing realization of the importance and limitation of C18 diacid, which ultimately raises interest in seeking new small-molecule alternatives.[43,44] It is known that many chemical drugs, such as ibuprofen, can bind to albumin and prolong their circulatory half-lives.[45] In principle, these drugs could be used as functional alternatives to C18 diacid and prolong the half-life of bioactive peptides. However, most of these chemicals display very weak avidity to albumin ($K_D \sim 100\ \mu M$) and sometimes even lose binding affinity upon peptide conjugation.[46] The DNA-encoded chemical library has been applied to identify the small-molecule albumin binder.[47] The best candidate, 4-(*p*-iodophenyl)butyric acid, displays a K_D value of 3.3 μM to HSA, but its capability to protract peptides has not been evaluated yet.[47] In this study, we evaluate the potential of CBB as an alternative to the C18 diacid for GLP-1 peptide protraction. CBB is an FDA-approved drug with a well-documented clinical safety. Its chemical structure is distinct from lipids, which might overcome some limitations seen in C18 diacid, for example, the aqueous solubility in the weak basic buffer (Figure S5). Additionally, the zwitterionic structure of CBB protractor might be advantageous over the anionic C18 diacid for oral absorption.[48] Since CBB has a pan-interaction with many proteins, including mucous membranes, we may envision an interesting translocation of coomatides from the gut lumen to mucosa, which benefits the oral formulation of GLP-1.

Our data indicate that CBB has a binding affinity for albumin HSA higher than that of C18 diacid. The subsequent PK studies and glucose control experiments collectively demonstrate that CBB has a similar, even slightly better, promoting effect than C18 diacid in mouse models. However, there is ongoing appreciation that the PK of peptide protractors in rodents cannot correlate with their behavior in humans. For example, semaglutide displays much better PK parameters in humans than in rats because of the protractor's optimal affinity to albumin of human species.[49,50] Despite the comparable effect in mice as shown in Figure 6, two protractors might show disparity in peptide protractions to higher species, especially considering the good performance of the C18 diacid in humans. Meanwhile, the immune risk might be another concern. In spite of a good safety history, CBB, once conjugated to peptide, might act as a hapten to generate the complete antigen (hapten-carrier adduct), which can trigger an immune response.[51,52] More study is required to pave the way for CBB as a peptide protractor in medical use.

It is worth noting that CBB is different from the C18 diacid in the mechanism of peptide protraction. Albumin, such as HSA, might contain a defined pocket for the C18 diacid protractor, rendering a unique and specific binding to the carrier protein.[15,28] CBB, in contrast, is a nonspecific protractor

https://doi.org/10.1021/acs.jmedchem.4c02970
J. Med. Chem. XXXX, XXX, XXX−XXX

that may associate with all proteins it encounters. It might fulfill the task of peptide protraction by taking advantage of the predominant abundance of albumin in serum. Besides protraction, the nonspecific binding feature of the CBB protractor also contributes to the slow release of peptides from the SC depot. The scientific rationale stems from the presence of collagen-rich meshwork under the skin, which traps the CBB-conjugated peptides and promotes exchange with the microvessel fluid.[53] The BLI assay confirms the avidity of CBB to collagen protein in vitro. The delayed T_{max} peaks of PK in comparison to semaglutide are a reflection of the controlled peptide release by CBB protractor after SC administration. The slow release from depots, although it tends to slow the onset of effect (actually, we did not see it in Figure 6), is quite helpful in prolonging the duration of peptide action.

In summary, we have reported a new protractor CBB that can potentiate the GLP-1 peptide with long-term action and slow release from the SC depot. We describe the SAR of CBB/GLP-1 conjugates with various linkers and conjugation positions. The best candidate coomatide 13 demonstrates a dramatically increased stability and circulation half-life, which supports the long-term and robust control of blood glucose in db/db mouse models. Protraction mechanism studies based on BLI assay reveals that protractor CBB is different from the lipoid protractor C18 diacid (semaglutide) in aspects of binding specificity and protracting scenario, which renders it a new small-molecule protractor suitable for advanced peptide delivery.

EXPERIMENTAL SECTION

Materials. Fmoc-Gly-Wang resins were purchased from GL Biochemical Ltd. (Shanghai, China). Liraglutide, semaglutide, and collagen were purchased from Macklin Biotechnology Inc. (Shanghai, China). HSA was purchased from Sigma-Aldrich (St. Louis, USA). All other chemicals and solvents were generally purchased from commercial sources without further purification. The bright-Lumi Firefly Luciferase Assay Kit was purchased from Beyotime Biotechnology (Shanghai, China). Dulbecco's modified Eagle medium/nutrient mixture F-12 (DMEM/F12) medium, FBS, and other cell culture supplementary reagents were purchased from Procell Inc. (Wuhan, China).

Synthesis of Peptides. Coomatides 1−11 was prepared by standard solid phase peptide synthesis using the Fmoc strategy (Scheme S1). Resins used were Fmoc-Gly-Wang resins with loadings of 0.3−0.8 mmol/g. Fmoc-Lys (Mtt)−OH was incorporated at the 26th position in order to be used for the side chain derivatization. After peptide chain elongation, the Mtt group was removed by hexafluoroisopropanol: dichloromethane (3:1) for 1 h. Then the linker building blocks and CBB protractor (synthesis method is available in the Supporting Information method) were sequentially coupled on the side chain using the Fmoc strategy. Finally, the peptide was cleaved from the resin by TFA/phenol/water/triisopropylsilane (88:5:5:2) for 2 h, followed by ether precipitation and a wash. The coomatide analogues were purified by Thermo Ultimate 3000 using a C18-column (Agilent, 250 × 9.4 mm; 5 μm) in an acetonitrile/water/TFA elution system. The purity and identity of the product were established by high-performance liquid chromatography (HPLC) coupled with electrospray ionization MS (ESI-MS). The purity of the peptides was confirmed to be ≥95% for all coomatide analogues.

Coomatides 12−15 were prepared by a liquid semisynthesis approach (Scheme 1). Briefly, GLP-1 peptides (TGPeptide Biological, Nanjing) were reacted with CBB-PEG8-NHS in a DMF/0.1 M $NaHCO_3$ solution mixture (4/1, v/v) for 1 h. The coomatide analogues were purified from the reaction by reverse phase HPLC. Detailed procedures are provided in the Supporting Information.

Construction of HEK293/CRE-Luc/GLP-1R Stable Cell Line. The donor vector pAAVS1-GLP-1R-CRE-Luc, bearing a GLP-1R gene and a CRE-Luc reporter gene, was constructed by molecular cloning. This vector plus the CRISPR guide vector pCas-Guide-AAVS1 was then cotransfected into HEK-293 cells using the jetPRIME transfection reagent (Polyplus, France). 72 h after transfection, the cells were subjected to a selective pressure of 200 μg/mL G418. After 4 weeks of selection, the cells were serially diluted to an extremely low density and plated to 96-well plates for the single-cell cloning. The clone cells were amplified, evaluated, and stored in liquid nitrogen for later use.

In Vitro Function Assay. In vitro functional assessment of peptides was performed on the HEK293/CRE-Luc/GLP-1R stable cell line. Cells were plated into 96-well white opaque plates at a density of 20,000 cells/well (100 μL). After overnight culture, the medium was changed to the assay buffer containing the peptide compounds (final concentration from 1×10^{-7} to 1 × 10 ng/mL). Depending on the experimental condition, the assay buffer can be DMEM/F12 containing no serum, 2% has, or 10% FBS. Plate was incubated for 8 h at 37 °C with 5% CO_2. A 100 μL portion of Bright-Lumi reagent was added into the wells and incubated according to the manufacturer's protocol. The plate was read in an Infinite M Plex microplate reader (Tecan, Switzerland). Data was analyzed using GraphPad Prism version 9, and EC_{50} values were analyzed using a nonlinear regression equation: agonist vs response-variable slope (four parameters).

Plasma Stability Assay. Plasma was obtained from SD rats (male, body weight 180−250 g) and used fresh for the study. Aqueous solution (0.1 M $NaHCO_3$) of semaglutide (5 mg/mL), coomatide 13 (5 mg/mL), and (G8R26)GLP-1(7−36) (5 mg/mL) was mixed with rat plasma (1/9, v/v) and incubated at 37 °C. The aliquot (25 μL) was sampled at 0, 6, 12, 24, 48, and 96 h. The plasma protein was precipitated by mixing with 5× volume of acetonitrile/methanol (5/1, v/v). The mixture was centrifuged at 12000 rpm for 15 min, and the supernatant was analyzed via the LC-40D HPLC system (SHIMADZU, Japan).

In Vivo PKs. PK studies were conducted in BALB/c mice and SD rats, respectively. To profile the PK in mice, semaglutide and coomatide 13 were IV or SC injected into BALB/c male mice with a dose of 0.5 mg/kg. Blood samples were collected from tail vein at selected time points (0, 2, 4, 6, 12, 24, and 48 h). The samples were centrifuged for 5 min (12,000 rpm) at 4 °C. The supernatant plasma was transferred and frozen immediately into −80 °C until quantification by LC−MS/MS. The LC−MS/MS instrumentation is supplemented in the Supporting Information.

To study PK in rats, male SD rats (body weight 180−220 g) were used and kept in standard cages. After 1 week of acclimatization, semaglutide and coomatide 13 were IV or SC administrated at the dose of 1 mg/kg. Blood samples were collected from the tail vein at selected time points (0, 2, 4, 6, 12, 24, and 48 h). Blood samples were collected in the EDTA tubes and centrifuged for 5 min (12,000 rpm) at 4 °C. The supernatant plasma was transferred and frozen immediately into −80 °C for LC−MS/MS.

Fluorescence Imaging In Vivo. Male BALB/c mice (8 weeks of age) were randomly divided into 3 groups (n = 3). Control (sulfo-Cy7 acid), semaglutide (sulfo-Cy7 labeled), and coomatide 13 (sulfo-Cy7-labeled) were injected into mice of each group via tail vein at the doses of 50 nmol/kg. Then the mice were euthanized 2, 6, and 12 h after administration. The abdomens of the mice were opened and imaged using the in vivo Xtreme II imaging system (Bruker, UK). For ex vivo tracking, the major organs (heart, liver, spleen, lung, and kidney) were harvested and imaged.

To track the SC absorption, male BALB/c-nu mice (8 weeks of age) were randomly divided into 2 groups (n = 3). Semaglutide (sulfo-Cy7-labeled) and coomatide 13 (sulfo-Cy7-labeled) were SC injected into mice of each group with a volume of 20 μL. The diffusion of peptide under the skin was recorded using either the

https://doi.org/10.1021/acs.jmedchem.4c02970
J. Med. Chem. XXXX, XXX, XXX−XXX

camera or the in vivo Xtreme II imaging system (Bruker, UK) at 0, 3, 6, and 12 h post injection.

Biolayer Interferometry Assay. ForteBio Octet Red96e biosensor system (ForteBio, Germany) equipped with amine reactive second-generation (AR2G) biosensors was used to study the interaction of semaglutide and coomatide 13 with the different kinds of proteins—HSA, GLP-1, and collagen type I. HSA, GLP-1, and collagen were dissolved separately in the sodium acetate buffer (pH = 5) to a working concentration of 50 μg/mL for use. After 10 min of activation in water, the AR2G biosensors were activated with EDCI and sulfo-NHS for 5 min. Then HSA, GLP-1, and collagen were immobilized onto the AR2G biosensors for 10 min, respectively. The unreacted groups in the biosensor were then quenched with 1 M ethanolamine for 5 min. After washing with PBS buffer for 3 min to get a smooth baseline, the biosensors fixed with different proteins were immerged into the CBB (0, 0.5, 1, 2, 3, and 4 μM) or semaglutide (0, 0.5, 1, 2, and 5 μM) or coomatide 13 (0, 0.5, 1, 2, and 5 μM) solution to associate for 3 min and then dissociated in PBS for 5 min. The data were analyzed using ForteBio Data Analysis 11.1 software with a standard 1/1 binding model.

Dose-Dependent Response in db/db Mice. Male db/db mice (8 weeks of age, Huachuang Sino, China) with blood glucose levels over 10 mM were kept in standard cages. They were given free access to standard chow and water. After 1 week of acclimatization, the mice were allocated to 7 groups (n = 5). Coomatide 13 was injected subcutaneously at the dose ranging from 3−600 nmol/kg. Blood glucose levels were assessed at the time points 0, 1, 2, 4, 6, 12, 24, 48, and 96 h after dosing. Samples for the measurement of blood glucose were obtained from the tail tip capillaries of the mice. The mice were accustomed to this procedure prior to the experiment. During the experiment, mice were kept free to move in their cages. All the experimental procedure was approved by the Institutional Animal Care and Use Committee of Wuhan University.

Glucose Control by Single-Dose in db/db Mice. Male db/db mice (8 weeks of age) were allocated to 4 groups randomly. Vehicle control, semaglutide, coomatide 13, and (G8R6)GLP-1(7−36) were SC injected at a fixed volume of 50 μL. Tail blood glucose levels were determined with tail tip capillary of the mice at 0, 1, 2, 4, 6, 12, 24, 36, 48, 60, 72, 96, 120, and 144 h after dosing. The glucose control in db/db mice was tested in a single-dose regimen of 100 and 600 nmol/kg, respectively. The blood glucose profiles were represented as the mean ± SD versus time (n = 5).

Glucose Control by Repeated Dose in db/db Mice. Male db/db mice were allocated to 2 groups. Semaglutide and coomatide 13 were injected subcutaneously with a dose of 600 nmol/kg (3 injections, once every 48 h). Tail blood glucose levels were determined with a one-touch glucometer at 0, 2, 6, 12, 24, and 48 h post every injection. The blood glucose profiles were represented as the mean ± SD versus time (n = 5).

Intraperitoneal Glucose Tolerance Test. Male db/db mice (n = 3) were subjected to 16 h of fasting and injected with glucose (1 g/kg) intraperitoneally. Vehicle (50 μL, PBS), semaglutide (100 nmol/kg), and coomatide 13 (100 nmol/kg) were SC injected 30 min prior to the glucose administration. Tail blood glucose levels were determined with a one-touch glucometer at 0.5 h before and at 0, 0.25, 0.5, 1, and 2 h after the glucose challenge.

Acute Oral Glucose Tolerance Test. Male db/db mice (n = 3) were subjected to 16 h of fasting, and glucose (1.5 g/kg) was taken orally using a gavage needle. Vehicle (50 μL, PBS), semaglutide (100 nmol/kg), and coomatide (100 nmol/kg) were subcutaneously injected 3 h prior to the glucose load. Tail blood glucose levels were determined with a one-touch glucometer at 3 h before and at 0.25, 0.5, 1, and 2 h after the glucose administration.

Feeding Test. Male db/db mice (aged 8 weeks) were subjected to 16 h of fasting prior to the commencement of the experiment. Subsequently, vehicle (50 μL, PBS), semaglutide (100 nmol/kg), and coomatide (100 nmol/kg) were subcutaneously administrated, and the food (100 g) was put back into the cage immediately. The remaining chow was weighed at 4, 6, 12, 24, 36, and 48 h. The cumulative food intake was calculated and plotted against time (n = 3).

Statistical Analysis. Statistical analysis was performed using GraphPad Prism 9.3.0. Data were presented as the mean ± SD. P-values were calculated using the two-way ANOVA with Tukey's multiple comparison test. $P < 0.05$ was considered to be statistically significant.

■ ASSOCIATED CONTENT

Supporting Information

The Supporting Information is available free of charge at https://pubs.acs.org/doi/10.1021/acs.jmedchem.4c02970.

Synthetic methods for all compounds, HPLC conditions, LC/MS methods, and supplementary mass and HPLC spectra (PDF)

Molecular formulation strings (CSV)

■ AUTHOR INFORMATION

Corresponding Author

Wanyi Tai − *Department of Pharmaceutical Engineering, School of Pharmaceutical Sciences, Wuhan University, Wuhan, Hubei 430071, China;* orcid.org/0000-0003-3589-8263; Email: wanyi-tai@whu.edu.cn

Authors

Weina Jing − *Department of Pharmaceutical Engineering, School of Pharmaceutical Sciences, Wuhan University, Wuhan, Hubei 430071, China*

Lei Peng − *Department of Pharmaceutical Engineering, School of Pharmaceutical Sciences, Wuhan University, Wuhan, Hubei 430071, China*

Shiwei Song − *Department of Pharmaceutical Engineering, School of Pharmaceutical Sciences, Wuhan University, Wuhan, Hubei 430071, China*

Jiaqi Liu − *Department of Pharmaceutical Engineering, School of Pharmaceutical Sciences, Wuhan University, Wuhan, Hubei 430071, China*

Complete contact information is available at: https://pubs.acs.org/10.1021/acs.jmedchem.4c02970

Author Contributions

The manuscript was written through contributions of all authors. All authors have given their approval to the final version of the manuscript.

Notes

The authors declare no competing financial interest.

All the animal studies were performed in compliance with the guidelines of the Chinese Regulations for the Administration of Affairs Concerning Experimental Animals and the Institutional Animal Care and Use Committee of Wuhan University. The approval numbers are WQ20210410 and WP20210588.

■ ACKNOWLEDGMENTS

This work was financially supported by the National Key R&D Program of China (grant no. 2021YFA0909900) and the National Natural Science Foundation of China (82273860).

■ ABBREVIATIONS

BLI, bio-layer interferometry; CBB, coomassie brilliant blue; CRE, cAMP response element; Fc, fragment crystallizable; GLP-1R, glucagon-like peptide 1 receptor; RP-HPLC, reverse-phase high performance liquid chromatography; SPPS, solid-

phase peptide synthesis; SAR, structure−activity relationship; SD rats, Sprague−Dawley rats

REFERENCES

(1) Madsen, T. D.; Hansen, L. H.; Hintze, J.; Ye, Z.; Jebari, S.; Andersen, D. B.; Joshi, H. J.; Ju, T.; Goetze, J. P.; Martin, C.; et al. An atlas of O-linked glycosylation on peptide hormones reveals diverse biological roles. *Nat. Commun.* **2020**, *11* (1), 4033.

(2) Wang, L.; Wang, N.; Zhang, W.; Cheng, X.; Yan, Z.; Shao, G.; Wang, X.; Wang, R.; Fu, C. Therapeutic peptides: current applications and future directions. *Signal Transduction Targeted Ther.* **2022**, *7* (1), 48.

(3) Hutchinson, J. A.; Burholt, S.; Hamley, I. W. Peptide hormones and lipopeptides: from self-assembly to therapeutic applications. *J. Pept. Sci.* **2017**, *23* (2), 82−94.

(4) Muttenthaler, M.; King, G. F.; Adams, D. J.; Alewood, P. F. Trends in peptide drug discovery. *Nat. Rev. Drug Discovery* **2021**, *20* (4), 309−325.

(5) Sohrabi, C.; Foster, A.; Tavassoli, A. Methods for generating and screening libraries of genetically encoded cyclic peptides in drug discovery. *Nat. Rev. Chem* **2020**, *4* (2), 90−101.

(6) Fetse, J.; Kandel, S.; Mamani, U.-F.; Cheng, K. Recent advances in the development of therapeutic peptides. *Trends Pharmacol. Sci.* **2023**, *44* (7), 425−441.

(7) Tai, W.; Gao, X. Functional peptides for siRNA delivery. *Adv. Drug Delivery Rev.* **2017**, *110−111*, 157−168.

(8) Margus, H.; Padari, K.; Pooga, M. Cell-penetrating Peptides as Versatile Vehicles for Oligonucleotide Delivery. *Mol. Ther.* **2012**, *20* (3), 525−533.

(9) Mahari, S.; Shahdeo, D.; Banga, I.; Choudhury, S., et al. Clinical and preclinical data on therapeutic peptides. In *Peptide and Peptidomimetic Therapeutics*; Qvit, N., Rubin, S. J. S., Eds.; Academic Press, 2022; Chapter 27, pp 657−688.

(10) Sharma, K.; Sharma, K. K.; Sharma, A.; Jain, R. Peptide-based drug discovery: Current status and recent advances. *Drug Discovery Today* **2023**, *28* (2), 103464.

(11) He, M. M.; Zhu, S. X.; Cannon, J. R.; Christensen, J. K.; et al. Metabolism and Excretion of Therapeutic Peptides: Current Industry Practices, Perspectives, and Recommendations. *Drug Metab. Dispos.* **2023**, *51* (11), 1436−1450.

(12) Lau, J. L.; Dunn, M. K. Therapeutic peptides: Historical perspectives, current development trends, and future directions. *Bioorg. Med. Chem.* **2018**, *26* (10), 2700−2707.

(13) Mathur, D.; Prakash, S.; Anand, P.; Kaur, H.; Agrawal, P.; Mehta, A.; Kumar, R.; Singh, S.; Raghava, G. P. S. PEPlife: A Repository of the Half-life of Peptides. *Sci. Rep.* **2016**, *6* (1), 36617.

(14) Cavaco, M.; Valle, J.; Flores, I.; Andreu, D.; et al. Estimating peptide half-life in serum from tunable, sequence-related physicochemical properties. *Clin. Transl. Sci.* **2021**, *14* (4), 1349−1358.

(15) Zorzi, A.; Middendorp, S. J.; Wilbs, J.; Deyle, K.; Heinis, C. Acylated heptapeptide binds albumin with high affinity and application as tag furnishes long-acting peptides. *Nat. Commun.* **2017**, *8*, 16092.

(16) Angelini, A.; Morales-Sanfrutos, J.; Diderich, P.; Chen, S.; et al. Bicyclization and tethering to albumin yields long-acting peptide antagonists. *J. Med. Chem.* **2012**, *55* (22), 10187.

(17) Dennis, M. S.; Zhang, M.; Meng, Y. G.; Kadkhodayan, M.; et al. Albumin binding as a general strategy for improving the pharmacokinetics of proteins. *J. Biol. Chem.* **2002**, *277* (38), 35035.

(18) Yu, M.; Benjamin, M. M.; Srinivasan, S.; Morin, E. E.; et al. Battle of GLP-1 delivery technologies. *Adv. Drug Delivery Rev.* **2018**, *130*, 113−130.

(19) Wan, W.; Qin, Q.; Xie, L.; Zhang, H.; et al. GLP-1R Signaling and Functional Molecules in Incretin Therapy. *Molecules* **2023**, *28* (2), 751.

(20) Drucker, D. J. The GLP-1 journey: from discovery science to therapeutic impact. *J. Clin. Invest.* **2024**, *134*(2), e175634.

(21) Hirsch, I. B. The Future of the GLP-1 Receptor Agonists. *Jama* **2019**, *321* (15), 1457−1458.

(22) Bech, E. M.; Pedersen, S. L.; Jensen, K. J. Chemical Strategies for Half-Life Extension of Biopharmaceuticals: Lipidation and Its Alternatives. *ACS Med. Chem. Lett.* **2018**, *9* (7), 577−580.

(23) Lau, J.; Bloch, P.; Schäffer, L.; Pettersson, I.; et al. Discovery of the Once-Weekly Glucagon-Like Peptide-1 (GLP-1) Analogue Semaglutide. *J. Med. Chem.* **2015**, *58* (18), 7370−7380.

(24) Kjeldsen, T. B.; Hubálek, F.; Hjørringgaard, C. U.; Tagmose, T. M.; et al. Molecular Engineering of Insulin Icodec, the First Acylated Insulin Analog for Once-Weekly Administration in Humans. *J. Med. Chem.* **2021**, *64* (13), 8942−8950.

(25) Pechenov, S.; Revell, J.; Will, S.; Naylor, J.; Tyagi, P.; Patel, C.; Liang, L.; Tseng, L.; Huang, Y.; Rosenbaum, A. I.; et al. Development of an orally delivered GLP-1 receptor agonist through peptide engineering and drug delivery to treat chronic disease. *Sci. Rep.* **2021**, *11* (1), 22521.

(26) Coskun, T.; Sloop, K. W.; Loghin, C.; Alsina-Fernandez, J.; et al. LY3298176, a novel dual GIP and GLP-1 receptor agonist for the treatment of type 2 diabetes mellitus: From discovery to clinical proof of concept. *Mol. Metab.* **2018**, *18*, 3−14.

(27) Østergaard, S.; Paulsson, J. F.; Kofoed, J.; Zosel, F.; Olsen, J.; Jeppesen, C. B.; Spetzler, J.; Ynddal, L.; Schleiss, L. G.; Christoffersen, B. Ø.; et al. The effect of fatty diacid acylation of human PYY3−36 on Y2 receptor potency and half-life in minipigs. *Sci. Rep.* **2021**, *11* (1), 21179.

(28) Wang, Y.; Lomakin, A.; Kanai, S.; Alex, R.; et al. The molecular basis for the prolonged blood circulation of lipidated incretin peptides: Peptide oligomerization or binding to serum albumin? *J. Controlled Release* **2016**, *241*, 25−33.

(29) Venanzi, M.; Savioli, M.; Cimino, R.; Gatto, E.; et al. A spectroscopic and molecular dynamics study on the aggregation process of a long-acting lipidated therapeutic peptide: the case of semaglutide. *Soft Matter* **2020**, *16* (44), 10122−10131.

(30) Brichtová, E. P.; Krupová, M.; Bouř, P.; Lindo, V.; et al. Glucagon-like peptide 1 aggregates into low-molecular-weight oligomers off-pathway to fibrillation. *Biophys. J.* **2023**, *122* (12), 2475−2488.

(31) Enaida, H.; Hisatomi, T.; Hata, Y.; Ueno, A.; Goto, Y.; Yamada, T.; Kubota, T.; Ishibashi, T. Brilliant blue G selectively stains the internal limiting membrane/brilliant blue G-assisted membrane peeling. *Retina* **2006**, *26* (6), 631.

(32) Georgiou, C. D.; Grintzalis, K.; Zervoudakis, G.; Papapostolou, I. Mechanism of Coomassie brilliant blue G-250 binding to proteins: a hydrophobic assay for nanogram quantities of proteins. *Anal. Bioanal. Chem.* **2008**, *391* (1), 391−403.

(33) Knudsen, L. B.; Nielsen, P. F.; Huusfeldt, P. O.; Johansen, N. L.; et al. Potent derivatives of glucagon-like peptide-1 with pharmacokinetic properties suitable for once daily administration. *J. Med. Chem.* **2000**, *43* (9), 1664−1669.

(34) Madsen, K.; Knudsen, L. B.; Agersoe, H.; Nielsen, P. F.; et al. Structure-activity and protraction relationship of long-acting glucagon-like peptide-1 derivatives: importance of fatty acid length, polarity, and bulkiness. *J. Med. Chem.* **2007**, *50* (24), 6126.

(35) Peng, D.; Li, Y.; Si, L.; Zhu, B.; et al. A two-step method preparation of semaglutide through solid-phase synthesis and inclusion body expression. *Protein Expr. Purif.* **2024**, *219*, 106477.

(36) Wu, Z.; Li, Y.; Zhang, L.; Ding, Z.; et al. Microbial production of small peptide: pathway engineering and synthetic biology. *Microb. Biotechnol.* **2021**, *14* (6), 2257−2278.

(37) Vahl, T. P.; Paty, B. W.; Fuller, B. D.; Prigeon, R. L.; et al. Effects of GLP-1-(7−36)NH2, GLP-1-(7−37), and GLP-1- (9−36)NH2 on intravenous glucose tolerance and glucose-induced insulin secretion in healthy humans. *J. Clin. Endocrinol. Metab.* **2003**, *88* (4), 1772.

(38) Sebokova, E.; Christ, A. D.; Wang, H.; Sewing, S.; et al. Taspoglutide, an analog of human glucagon-like Peptide-1 with enhanced stability and in vivo potency. *Endocrinology* **2010**, *151* (6), 2474−2482.

https://doi.org/10.1021/acs.jmedchem.4c02970
J. Med. Chem. XXXX, XXX, XXX−XXX

(39) Jones, G. B.; Collins, D. S.; Harrison, M. W.; Thyagarajapuram, N. R.; Wright, J. M. Subcutaneous drug delivery: An evolving enterprise. *Sci. Transl. Med.* **2017**, *9* (405), No. eaaf9166.
(40) Li, W.; Tang, J.; Lee, D.; Tice, T. R.; et al. Clinical translation of long-acting drug delivery formulations. *Nat. Rev. Mater.* **2022**, *7* (5), 406−420.
(41) Bokvist, K.; Ding, Y.; Landschulz, W. H.; Sinha, V.; et al. Gastrin analogue administration adds no significant glycaemic benefit to a glucagon-like peptide-1 receptor agonist acutely or after washout of both analogues. *Diabetes Obes. Metab.* **2019**, *21* (7), 1606−1614.
(42) Ding, S.; Song, M.; Sim, B.-C.; Gu, C.; et al. Multivalent Antiviral XTEN−Peptide Conjugates with Long in Vivo Half-Life and Enhanced Solubility. *Bioconjugate Chem.* **2014**, *25* (7), 1351−1359.
(43) Liu, Y.; Wang, G.; Zhang, H.; Ma, Y.; et al. Stable Evans Blue Derived Exendin-4 Peptide for Type 2 Diabetes Treatment. *Bioconjugate Chem.* **2016**, *27* (1), 54−58.
(44) Bech, E. M.; Martos-Maldonado, M. C.; Wismann, P.; Sørensen, K. K.; et al. Peptide Half-Life Extension: Divalent, Small-Molecule Albumin Interactions Direct the Systemic Properties of Glucagon-Like Peptide 1 (GLP-1) Analogues. *J. Med. Chem.* **2017**, *60* (17), 7434−7446.
(45) Ghuman, J.; Zunszain, P. A.; Petitpas, I.; Bhattacharya, A. A.; et al. Structural Basis of the Drug-binding Specificity of Human Serum Albumin. *J. Mol. Biol.* **2005**, *353* (1), 38−52.
(46) Bocedi, A.; Notaril, S.; Narciso, P.; Bolli, A.; et al. Binding of anti-HIV drugs to human serum albumin. *IUBMB Life* **2004**, *56* (10), 609−614.
(47) Dumelin, C. E.; Trüssel, S.; Buller, F.; Trachsel, E.; et al. A portable albumin binder from a DNA-encoded chemical library. *Angew. Chem., Int. Ed.* **2008**, *47* (17), 3196−3201.
(48) Manallack, D. T.; Prankerd, R. J.; Yuriev, E.; Oprea, T. I.; et al. The significance of acid/base properties in drug discovery. *Chem. Soc. Rev.* **2013**, *42* (2), 485−496.
(49) Jensen, L.; Helleberg, H.; Roffel, A.; van Lier, J. J.; et al. Absorption, metabolism and excretion of the GLP-1 analogue semaglutide in humans and nonclinical species. *Eur. J. Pharm. Sci.* **2017**, *104*, 31−41.
(50) Lee, T. S.; Park, E. J.; Choi, M.; Oh, H. S.; et al. Novel LC-MS/MS analysis of the GLP-1 analog semaglutide with its application to pharmacokinetics and brain distribution studies in rats. *J. Chromatogr. B* **2023**, *1221*, 123688.
(51) Lemus, R.; Karol, M. H. Conjugation of haptens. *Methods Mol. Med.* **2008**, *138*, 167−182.
(52) Jalah, R.; Torres, O. B.; Mayorov, A. V.; Li, F.; et al. Efficacy, but not antibody titer or affinity, of a heroin hapten conjugate vaccine correlates with increasing hapten densities on tetanus toxoid, but not on CRM197 carriers. *Bioconjugate Chem.* **2015**, *26* (6), 1041−1053.
(53) Chen, W.; Yung, B. C.; Qian, Z.; Chen, X. Improving long-term subcutaneous drug delivery by regulating material-bioenvironment interaction. *Adv. Drug Delivery Rev.* **2018**, *127*, 20−34.

https://doi.org/10.1021/acs.jmedchem.4c02970
J. Med. Chem. XXXX, XXX, XXX−XXX